Computer Simulation Studies of the Adsorption of Water on a Metal Surface

E. Spohr and M. Wolfsberg

Institute for Surface and Interface Science and Department of Chemistry, University of California, Irvine, CA 92717

P. Bopp

Institut für Physikalische Chemie, Rheinisch-Westfälische Technische Hochschule, Aachen, FRG

Z. Naturforsch. **46a**, 174–182 (1991); received August 2, 1990

Dedicated to our teacher and friend Karl Heinzinger on the occasion of his sixtieth birthday

We report computer simulations of the adsorption process of water on a platinum (100) surface. At very low impact energies the sticking coefficient approaches unity in agreement with experimental evidence. The sticking coefficient for the bare surface decreases strongly with increasing impact energy already in the energy range <0.5 eV and also with increasing surface temperature. At all but the lowest impact energies the sticking coefficient increases drastically if the impact zone of the approaching molecule is in the vicinity of preadsorbed water molecule(s). The reason for this phenomenon is efficient energy transfer into water-water degrees of freedom and/or into the metal–O "bond" of the preadsorbed water molecules. In the present study, where surface diffusion does not play an important role because the impact zone is chosen to be close to the adsorbed molecule or cluster, hydrogen bonds are formed between incoming and preadsorbed molecules during approach and impact. Excess energy is transferred into the lattice within a few picoseconds leading to a two-dimensional hydrogen bonded water cluster.

1. Introduction

The interaction of water with metal surfaces has been the subject of a wide range of experimental work (for a review see [1]) and also of theoretical studies. Quantum chemical calculations [2–7] have been performed for single molecules adsorbed on specific sites of the surface. Experimental evidence, however, indicates that many of the adsorption phenomena observed, like multilayer formation and hydrogen bonding at submonolayer coverage, can only be understood as the consequence of the interplay between water-water and water-substrate interactions. In fact, only few experimental results have been published where the water coverage (the ratio of adsorbed water molecules to adsorption sites, i.e. surface lattice atoms) is below 0.05; this fact means that in most experiments typical water-water distances are not larger than 10 Å and even smaller if cluster formation occurs. In this context, computer simulations of the structure and dynamics provide a means to connect the information obtained from quantum chemical calculations (via the employed potential function) with the experimental many-particle situation.

To date, simulations of water near transition metal surfaces dealt mostly with the structure and dynamics of equilibrium systems like partially filled adlayers [8] and extended laminae [9–11] of water sandwiched between two crystal faces. In the present study, we extend these studies to the investigation of the dynamics of the adsorption process itself. The goal is to build up an adsorbate layer (2-dimensional water cluster) or a 3-dimensional water cluster by successive deposition of molecules from the gas phase. Experimental deposition times are such that about one molecule per second hits a typical simulated surface area of about (20×20) Å^2. As the adsorption process itself and the subsequent energy relaxation are fast on this time scale (*vide infra*), the initial stages of the cluster formation can be studied separately by performing independent trajectory calculations for a water molecule approaching a surface with n ($n=0, 1, 2, 5$ in the present study) preadsorbed molecules.

In Section 2, we briefly sketch the properties of the potential hypersurface; the details of the trajectory calculations follow in Section 3. The energy dependence of the sticking coefficient on the bare surface

Reprint requests to Dr. P. Bopp, Institut für Physikalische Chemie, Technische Hochschule Aachen, D-5100 Aachen.

0932-0784 / 91 / 0100-0174 $ 01.30/0. – Please order a reprint rather than making your own copy.

and the transfer of initial translational energy into the substrate and coadsorbate degrees of freedom are discussed in Section 4.

2. Potential Functions

Two interaction potential surfaces are used in the present work. The first one is the same as that used in previous studies [9–11]. A flexible water model is used to describe the water-water interactions [12] together with a set of pairwise additive platinum-oxygen and platinum-hydrogen potential functions and nearest-neighbor harmonic platinum-platinum interactions [13]. Some properties of this potential surface (called I) are collected in Table 1.

As was pointed out earlier [11], the water-platinum potential function I fails to reproduce the experimental frequency of the metal-water stretching mode [14]. Hence, an alternate potential surface with a higher metal-oxygen force constant was designed (model II) which is parametrized in terms of respective atom-atom distances r and projections of those distances on the surface plane ϱ as

$$V_{H_2O\text{-metal}} = \sum_{\substack{\text{metal}\\ \text{atoms i}}} \{\Phi_O(r_{O\text{-i}}, \varrho_{O\text{-i}}) + \Phi_H(r_{H_1\text{-i}}) + \Phi_H(r_{H_2\text{-i}})\} \tag{1}$$

with

$$\begin{aligned}\Phi_O(r, \varrho) = {} & 1.27[1 - 1.75 \exp\{-2.54(r-2.08)\}] \\ & \cdot \exp\{-0.41\,\varrho^2\} \\ & + 0.20[1 - 0.02 \exp\{-1.56(r-2.31)\}] \\ & \cdot [1 - \exp\{-0.41\,\varrho^2\}] \\ & + 10 \exp\{-8(z-1)\} \exp\{-0.4\,\varrho^2\}\end{aligned} \tag{2}$$

and

$$\Phi_H(r) = 1.71 \exp\{-1.28\,r\}\,. \tag{3}$$

Φ_O and Φ_H are in units of 10^{-19} J and the distances r and the projection ϱ of the distance on the surface plane are in Ångstrom units. Φ_H is identical with that of potential model I. This potential has a very small barrier of about 0.025 eV at $z \approx 4$ Å. Since the impact energies for this potential were larger than the barrier height, we don't expect this barrier height to have an effect on the calculations.

The full lines in Figs. 1 a and b show the variation of the total water crystal interaction energy above the on-top site of a Pt(100) surface of a crystal slab (*vide infra*) as a function of the perpendicular distance z of the oxygen atom from the surface for models I and II, respectively. Potential function I leads to a (coverage dependent) water binding energy between about 45 kJ/mol (at $\Theta = 0.2$) and about 60 kJ/mol at and beyond monolayer coverage [15]. This result compares favorably with the measured binding energy of 65 kJ/mol on Pt(111) [16]. Potential model II certainly overestimates the water-metal interaction energy (see also the discussion in Chapt. 4 of [1]) and thus serves as an extreme model for the system. It is apparent that the range of potential II is only about 1 water diameter. The dashed and dotted lines show the potential energy variation that a molecule feels when approaching the surface above an occupied on-top site (dashed) or above one of the nearest on-top sites surrounding the occupied site (dotted). The existence of a preadsorbed water molecule leads to stronger binding on the nearest site for both models and it generally leads to an increase of the range of the effective potential due to the long-ranged dipole-dipole interactions. The additional stabilization of the second molecule is of the order of 20 kJ/mol.

Table 1. Properties of the water-metal potential surfaces I and II. d is the perpendicular distance of the oxygen atom above the plane of surface lattice atoms, k_{zz} the metal-water (c.o.m.) force constant in the minimum energy configuration and $\nu_{O\text{-metal}}$ the frequency of the hindered translational motion perpendicular to the surface plane (obtained from a simulation of an isolated adsorbed water molecule in the on-top position at $T = 50$ K) and E the metal-water interaction energies in the energetically most favorable orientation (anti-dipole direction, where the dipole vector points away from the surface) on the specified sites.

	I	II
d/Å	2.3	2.3
k_{zz}/mdyn Å^{-1}	0.055	1.8
$\nu_{O\text{-metal}}$/cm^{-1}	80	395
adsorption site	on top	on top
orientation	anti-dipole	anti-dipole
$E_{on\text{-}top}$/kJ mol^{-1}	−35.7	−64.2
E_{bridge}/kJ mol^{-1}	−16.2	−50.7
E_{hollow}/kJ mol^{-1}	−12.0	−27.5

3. Details of the Simulation

The trajectory calculations were performed in the following way: Typically a crystal slab of 4 layers, each with 32 Pt atoms for the (100) surface, was equilibrated in the absence of any adsorbates for 6 picoseconds at the desired surface temperature T_S. In the presence of preadsorbed water this period was followed by two additional equilibration phases of 6 ps,

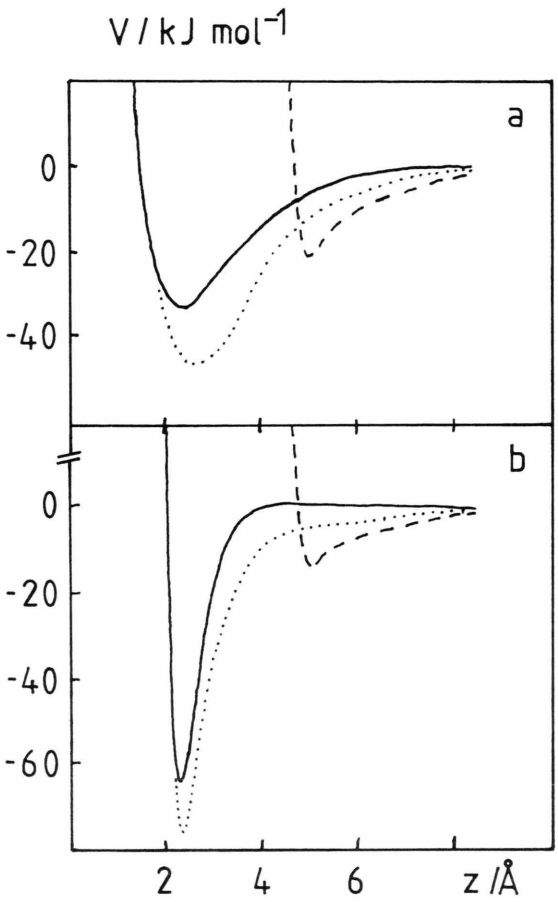

Fig. 1. Variation of the potential energy of a water molecule as a function of the perpendicular distance z from the surface for model I (a) and model II (b). Full line: an isolated molecule, in antidipole orientation (the dipole moment vector points perpendicularly away from the surface), above an on-top site. Dashed line: a water molecule, in antidipole orientation, above another molecule, preadsorbed in antidipole orientation on an on top-site. The two HOH planes form an angle of 90 degrees with each other. Dotted line: A molecule above one of the adsorption sites closets to a preadsorbed molecule. The HOH plane of the adsorbed molecule is perpendicular to the surface plane and one OH bond points towards the next adsorption site with the OH line parallel to the surface; the HOH plane of the incoming molecule is parallel to the surface plane and its dipole vector points away from the site of the first molecule.

first with and then without temperature adjustment, in which the adsorbate was inlcuded. The initial coordinates of the preadsorbed molecule(s) were fixed manually to be rather close to the desired equilibrium site and orientation. Initial conditions for the center of mass coordinates, the orientation, the internal coordinates, and the cartesian velocity components for all three atoms of the projectile molecule were chosen

Table 2. Definitions of the sets of initial conditions used in the various trajectory calculations. X_0, Y_0, and Z_0 are the coordinates of the center of mass of the projectile water molecule at zero time (in Å; see also Figure 4). In all runs the initial orientation of the incoming water molecules are chosen randomly from the complete orientational space. The OH distances and the HOH angle were chosen randomly from the intervals $0.9372 < r_{OH} < 0.9772$ Å and $100.52 < \alpha_{HOH} < 108.52°$, respectively. The equilibrium geometry of the water model is given by $r_{OH} = 0.9572$ Å and at $\alpha = 104.52°$. The internal velocities where chosen at random in cartesian space corresponding to a temperature of 50 K. This procedure leads, together with the potential energy due to the OH distance and HOH angle distortion, to an average initial energy of the molecule of 0.06 eV. N is the number of trajectories performed at a given value of the impact energy. Figure 4a depicts the x- and y-axes of the coordinate system for the tabulated quantities. The origin in z-direction is in the surface plane.

	Impact area	Z_0	N
A	whole crystal surface	10	200
B	$\lvert X_0\rvert, \lvert Y_0\rvert \leqq 3$	20	100
C	$\lvert X_0\rvert, \lvert Y_0\rvert \leqq 1.96$	20	100
D	$-6 \leqq X_0 \leqq -3;\ -3 \leqq Y_0 \leqq 3$	20	100

from homogeneous random distributions within the intervals specified in Table 2. Then the center of mass translational energy was adjusted to agree with the desired impact energy and impact direction (perpendicular approach to the surface was used in all simulations). The molecule thus had energy in the rotational and vibrational degrees of freedom. Newton's equations of motions were then solved with a fifth order Gear predictor-corrector [17] until one of the following termination criteria was met:

(a) The number of changes in the z component of the center of mass momentum of the molecule is 8 (equivalent to 5 impacts with the surface) after which the molecule was considered to be adsorbed.

(b) The distance of the center of mass from the surface is larger than 9 Å and simultaneously the kinetic energy for motion of the center of mass away from the surface is larger than the negative potential energy of the molecule from the water-water and water-platinum interactions at which time the molecule is considered to be scattered or desorbed.

(c) The simulation time exceeds 5 picoseconds. Usually less than 1% and in no case more than 3% of the trajectories were terminated according to this condition.

The time step length was 0.25 femtoseconds; this time step leads to an overall energy conservation of about 1 part in 10^7 per time step and a maximum total

Table 3. Sticking coefficients for the adsorption of water on a clean Pt(100) surface. T_s is the surface temperature and E_0 is the translational kinetic energy perpendicular to the surface. Set A of initial conditions was used in all runs (see Table 2). Uncertainties are estimated to be ± 0.05.

	T_s/K	p_{stick}							Remarks
		0.02	0.05	0.15	0.18	0.25	0.35	0.45 (E_0/eV)	
1	50	1.00	0.95	0.40	0.20	0.10	0.10	0.05	potential I, Pt mass
2	300	–	0.60	0.30	–	0.15	0.10	0.05	potential I, Pt mass
3	300	–	0.85	0.65	–	0.60	0.40	0.25	potential I, Ni mass
4	50	–	0.85	0.65	0.45	0.45	0.45	0.35	potential II, Pt mass
5	300	–	0.55	0.60	–	0.50	0.40	0.40	potential II, Pt mass
6	50	–	0.75	0.50	–	0.30	0.15	0.15	potential II divided by 2

energy change of about 0.05 kJ/mol over a whole trajectory. Periodic boundary conditions were employed parallel to the surface plane. Calculations with an increased number of layers or an increased number of lattice atoms per layer in a similar setup [18] show that the effect of system size is negligible within the limits of statistical uncertainty due to the finite number of trajectories, which was usually chosen to be 100 or 200 for a given system and impact energy.

4. Results

The results on the adsorption of water on the clean surface are summarized in Table 3. The sticking coefficient at a surface temperature of 50 K decreases strongly with increasing impact energy for both models (lines 1 and 4). The value obtained for an impact energy of 0.02 eV (which corresponds to about room temperature) at a surface temperature of 50 K is equal to the experimental values on several transition metal surfaces (see [1]). The sticking coefficient at low impact energy decreases with increasing surface temperature but appears to be rather independent of temperature at high impact energies (compare line 1 with line 2 and line 4 with line 5, respectively). It should be noted there that the sticking coefficient obtained from classical trajectory calculations is a lower bound because of the neglect of electronic deexcitation mechanisms like electron-hole formation (for a discussion see [19]).

The results in row 3 where the Pt mass has been changed to that of Ni (leaving everything else constant, including the metal-metal force constant and the lattice parameter), demonstrate that the small energy transfer into the platinum lattice can be increased by using a lighter mass. This effect can be qualitatively understood on the basis of a simple binary collision where the energy transfer decreases with increasing mass difference between the colliding species. It also demonstrates that an initial energy transfer into the lattice is important for the sticking behavior and that the energy is not only converted into water degrees of freedom (like e.g. rotation and vibration) and then released from there.

Table 4. Results for the sticking coefficient in the presence of n preadsorbed water molecules. p_{stick}(I) and p_{stick}(II) are the sticking coefficients obtained with models I and II, respectively. The initial conditions are those summarized in Table 2.

E_0/eV	n	p_{stick}(I)	p_{stick}(II)	Initial conditions
0.18	0	0.20	0.45	B
0.18	1	0.95	0.80	B
0.18	2	0.95	0.85	B
0.18	1	0.30	–	D
1.00	2	0.45	0.35	C
1.00	5	0.75	0.60	C

There are, however, characteristic differences between models I and II. The energy dependence is more pronounced for model I, yielding a higher adsorption probability at low and a lower adsorption probability at high impact energies than for model II. Line 6 in Table 3 suggests that the sticking coefficient at high energies depends on the binding energy (lower binding energy leads to a smaller sticking probability) whereas the sticking coefficient at low impact energies appears to have a more complex dependence on the potential energy surface parameters.

Table 4 shows that the sticking coefficient increases drastically if the approaching water molecules hit the surface in the vicinity of an adsorbed water molecule. For instance, the sticking coefficient at $E_0 = 0.18$ eV increases for model I from 0.20 to 0.95 if the impact zone is a (6×6) Å^2 area around an adsorbed water molecule. Qualitatively the same result is obtained with model II where the increase is from 0.45 to 0.80.

Addition of a second adsorbed water molecule in the impact zone does not lead to a significant increase in sticking. The effect of an isolated preadsorbed molecule is laterally not very long-ranged as can be seen from line 4 in Table 4. The sticking coefficient in the (3×6) Å^2 area next to the (6×6) Å^2 area of the trajectories in lines 1 through 3 is hardly increased relative to that of the bare surface. Note, from Fig. 4, that any preadsorbed molecules are, originally, in the area $|X_0|, |Y_0| \leqq 3$ Å.

As an example, Fig. 2a shows how 2 particular trajectories of an incoming water molecule differ after impact on the clean and the predosed surface. The initial orientation and impact parameter of the incoming water molecule are identical for both trajectories. In the case of the clean surface, the molecule collides twice with the surface. Just enough energy is lost from the translational mode during the first collision so that it is recaptured after 2.2 ps. In this second collision, the energy in the translational mode actually increases so that the molecule finally desorbs. However, if the molecule hits the surface in the vicinity of 2 preadsorbed molecules it is instantly adsorbed and performs the characteristic metal-oxygen stretching vibration just like the 2 preadsorbed molecules, but with a slightly larger amplitude.

We define the energy E_1 as

$$E_1 = T_1 + V_1, \tag{4}$$

where T_1 is the total kinetic energy of the water molecule and V_1 is the sum of all potential energy terms which involve molecule 1. It is apparent from Fig. 2b that energy is transferred into the lattice only during the two collisions ($\delta E_1 \approx -0.06$ eV and $\delta E_1 \approx -0.015$ eV in the first and second collision, respectively; full line). Energy transfer from the perpendicular translational mode into the kinetic energy of other water modes ($T_1 - T_Z$), T_Z being the center-of-mass kinetic energy perpendicular to the surface, is negative in the first ($\delta(T_1 - T_Z) \approx -0.185$ eV) and positive in the second collision ($\delta(T_1 - T_Z) \approx +0.065$ eV). Thus the final center-of-mass kinetic energy perpendicular to the surface exceeds the absolute magnitude of the water-metal binding energy and this particular trajectory desorbs. In the case of the predosed surface, the incoming molecule loses much more energy from $(T_Z + V_1)$ upon impact so that it sticks immediately (dashed curve). This result is due to the additional attraction by the other water molecules and dissi-

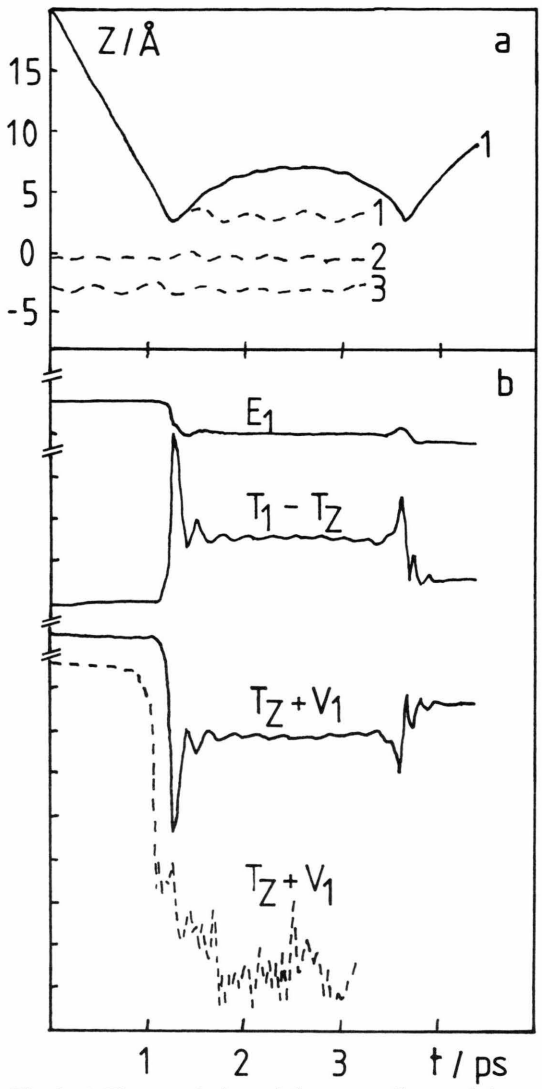

Fig. 2. a) Time evolution of the z-coordinate of the oxygen atom from particular trajectories for a water molecule colliding with a bare surface (full line) and for a water molecule colliding with a surface on which two water molecules are already preadsorbed (dashed line '1'). The corresponding distances of the preadsorbed molecules (labelled '2' and '3') are also given, offset by -3 and -6 Å, respectively. b) Time behaviour of the energy associated with the incoming molecule E_1, of the kinetic energy of the incoming water molecule in all but the perpendicular translational degree of freedom, $T_1 - T_Z$ for the case of the bare surface (full lines), and for the escape energy E_{esc} for the case of the bare surface (full line) and the surface with 2 preadsorbed water molecules (dashed line). The energy terms are defined in the text. The difference between two marks on the energy axis is 0.08 eV in all cases. The impact energy is 0.18 eV and the surface temperature is 50 K.

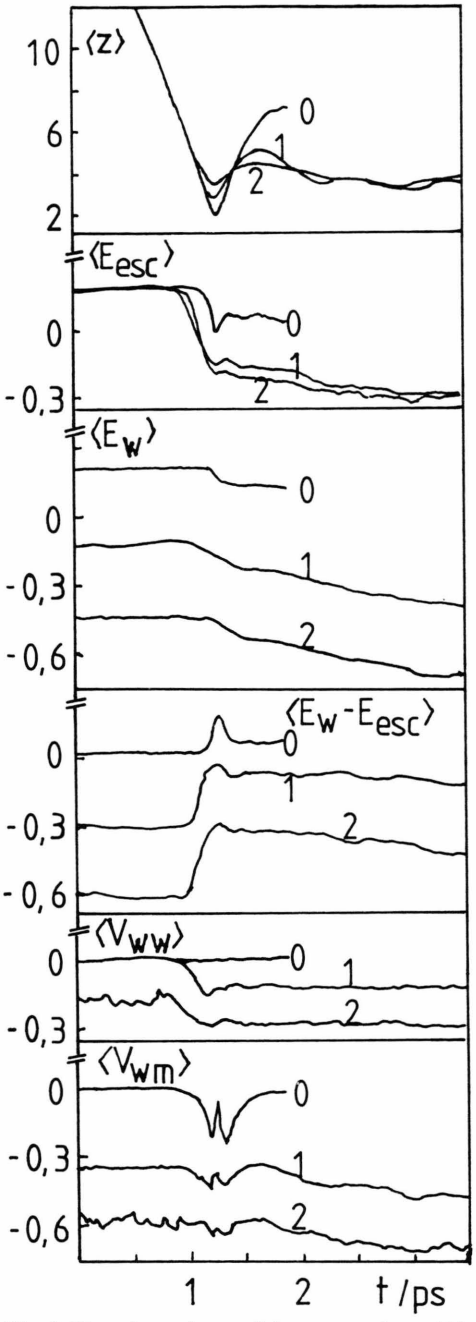

Fig. 3. Time dependence of the average (over 100 trajectories) perpendicular oxygen distance of the incoming molecule from the surface (top) $\langle Z \rangle$, and energy terms $\langle E_{esc} \rangle$, $\langle E_W \rangle$, $\langle E_W - E_{esc} \rangle$, $\langle V_{W\text{-}W} \rangle$, and $\langle V_{W\text{-}M} \rangle$ (from top to bottom) for water molecules hitting the bare surface and the surface with 1 or 2 preadsorbed molecules. The number labels on the curves denote the number of preadsorbed molecules. The impact energy is 0.18 eV and the surface temperature is 50 K.

pation of energy into their degrees of freedom (see below).

Figure 3 depicts, as a function of time, statistical averages of selected energy terms together with the average perpendicular distance of the oxygen atom of the incoming molecule from the surface for a collision energy of 0.18 eV and a surface temperature of 50 K. Note that the "average" distance of closest approach increases with increasing coverage because more and more molecules do not hit the surface directly, but another water molecule in the first collision. The energy of the incoming molecule (denoted as number 1) in the relevant degree of freedom for adsorption (center of mass motion perpendicular to the surface) is defined as $E_{esc} = T_Z + V_1$. The total energy of the water subsystem is defined as

$$E_W = \sum_{\text{water i}} T_i + V_{W\text{-}W} + V_{W\text{-}M}, \tag{5}$$

where $V_{W\text{-}W}$ and $V_{M\text{-}M}$ denote the total water-water and water-metal interaction energies, respectively (i.e. the sums over all respective pairs).

The energy of the incoming molecule $\langle E_{esc} \rangle$ changes stepwise during the collision of the water molecule with the bare surface. It is evident that the energy after impact is positive (on average) so that the majority of molecules is expected to scatter from the surface in agreement with the sticking coefficient of 0.20. In the case of both predosed surfaces, $\langle E_{esc} \rangle$ decreases significantly already before the turning point due to energy transfer into other degrees of freedom of the water subsystem (see $\langle E_W - E_{esc} \rangle$). The average value of $\langle E_{esc} \rangle$ after the collision is strongly negative for both predosed surfaces, which is the reason for the large sticking coefficient. The additional effect of the second water molecule on losses in $\langle E_{esc} \rangle$ is rather small but goes in the same direction as the effect of the first one. After the initial large energy loss in the collision process, $\langle E_{esc} \rangle$ gradually decreases.

The plot of $\langle E_W \rangle$ versus time shows that the energy transfer for the bare surface has a steplike character (see Figure 2). In the presence of preadsorbed water, the step washes out (partially because of a larger scatter of collision times, partly because energy is lost into other degrees of freedom of the water subsystem). Subsequently, energy is continuously lost out of the water subsystem. It is evident from $\langle E_W - E_{esc} \rangle$ that the energy "uptake" of the water subsystem increases with increasing number of preadsorbed molecules. The additional increase of $\langle E_W - E_{esc} \rangle$ results from dis-

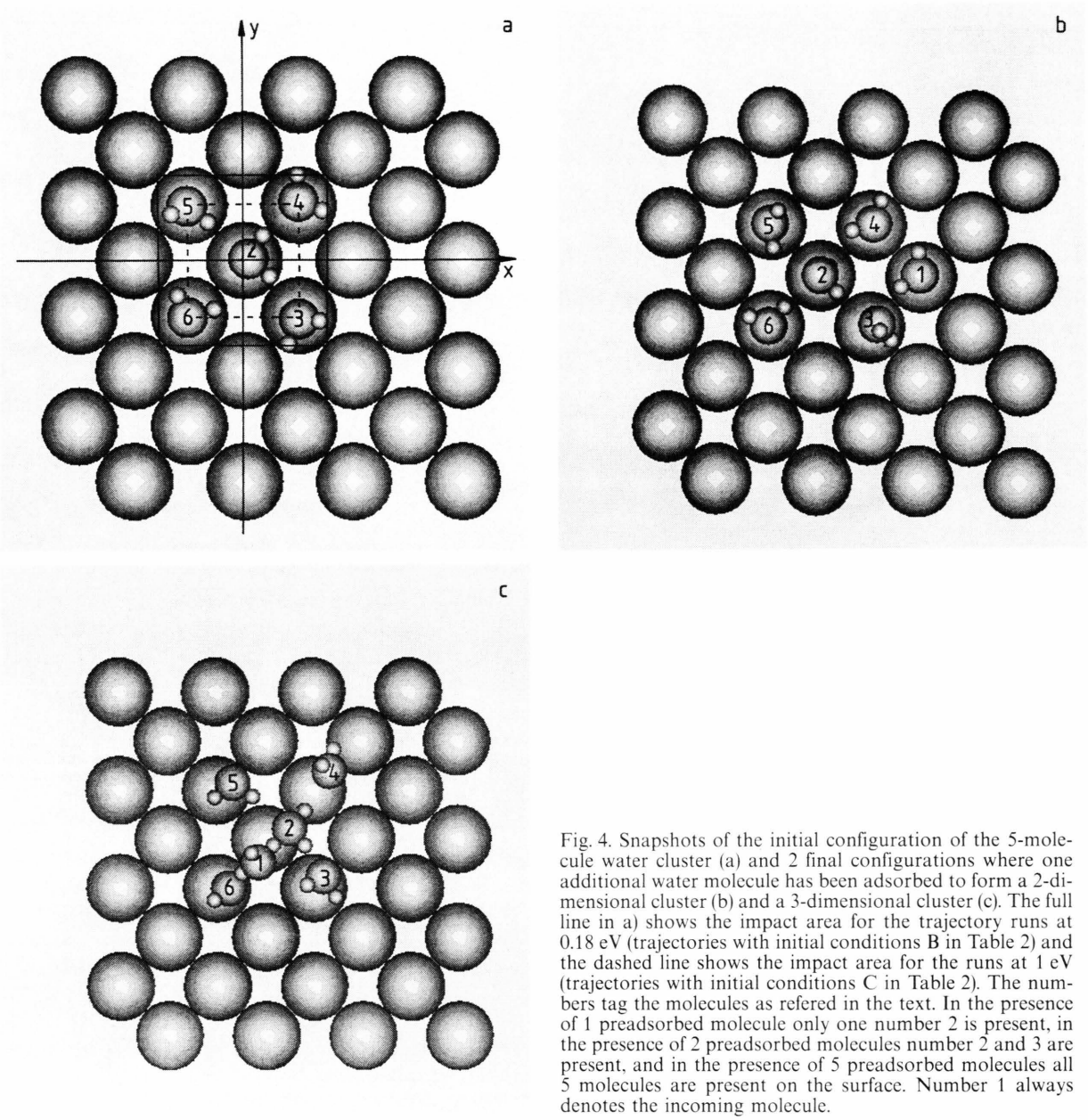

Fig. 4. Snapshots of the initial configuration of the 5-molecule water cluster (a) and 2 final configurations where one additional water molecule has been adsorbed to form a 2-dimensional cluster (b) and a 3-dimensional cluster (c). The full line in a) shows the impact area for the trajectory runs at 0.18 eV (trajectories with initial conditions B in Table 2) and the dashed line shows the impact area for the runs at 1 eV (trajectories with initial conditions C in Table 2). The numbers tag the molecules as refered in the text. In the presence of 1 preadsorbed molecule only one number 2 is present, in the presence of 2 preadsorbed molecules number 2 and 3 are present, and in the presence of 5 preadsorbed molecules all 5 molecules are present on the surface. Number 1 always denotes the incoming molecule.

torting the configurations of preadsorbed molecules from their equilibrium positions on the surface either through attractive water-water forces (hydrogen bonds) or after an impulsive collision when the preadsorbed molecules are pushed into the repulsive wall of the adsorption potential. $V_{W\text{-}W}$ indeed decreases considerably after impact for both predosed systems indicating the formation of additional hydrogen bonds. $V_{W\text{-}M}$ for the predosed surface decreases less drastically during the collision than in the case of the bare surface. This is due to the fact that not all molecules are stopped directly by the metal surface and also that the preadsorbed molecules are distorted to less favorably bonded configurations on the surface. The long-time decrease of this energy contribution shows that most of the long-term energy loss of the water subsystem results from the relaxation of water molecules into the most favorable adsorption sites and orientations.

The study has been extended to higher coverages. In order to observe additional sticking due to the higher coverage, the impact energy has been increased to 1 eV. At this energy, the sticking coefficient in the region defined by the dashed squares in Fig. 4 has been calculated in the presence of 2 water molecules (numbers 2 and 3 in Fig. 4) und 5 water molecules (numbers 2–6) on the corresponding adsorption sites. Again the adsorption probability increases considerably with increasing number of preadsorbed water molecules (lines 5 and 6 in Table 4). However, sticking at these high energies is generally less probable than last lower energies. In the presence of 2 preadsorbed molecules the excess energy is large enough to desorb all 3 molecules (for model I). Indeed, cases in which one, two, or three molecules are desorbed have been observed. The sticking coefficient in Table 4 is based on the sticking of the incoming molecule only and is thus too high. The fraction of trajectories in which all three water molecules remain adsorbed is only about 0.25. No desorption of the preadsorbed molecules has been observed in the case of the 5-molecule cluster. Here, apparently, the energy can usually be dissipated into water degrees of freedom without exceeding the binding energy of a single molecule.

Figure 4 shows the original water configuration on the substrate (a) and the results of 2 different trajectories, one leading to a 2-dimensional cluster (b) in which all molecules are adsorbed in the first layer above the surface and one to a 3-dimensional cluster (c) in which the incoming molecule is adsorbed in the second layer on top of the water cluster. The latter is stable on a time scale of about 2 picoseconds. Nevertheless, it is possible that it will evolve into a planar cluster. The number of studied trajectories is too small to allow a prediction whether 2-D or 3-D clusters are most likely to occur. Thermal desorption measurements [16] show the existence of two desorption peaks before saturation of the metal-bonded desorption peak; this result indicates that water forms multilayers before all adsorption sites are filled.

5. Conclusions

Water forms a relatively weak bond to transition metals. Our results show that the adsorption probability (sticking coefficient) is strongly energy dependent for two quite extreme choices of the water-metal potential function. The sticking coefficient is about unity in agreement with experimental data for impact energies characteristic of room temperature. Clearly, experimental studies at higher energies are desirable, expecially as the quantitative differences found for the two models suggest that the measurement of the energy dependence of the sticking coefficient would lead to further information about the water-metal potential energy surface.

The sticking probability is drastically increased at hyperthermal energies if preadsorbed water molecules are present. The reason for this result is that new degrees of freedom for very efficient transfer within the water adsorbate system become available. This effect depends apparently more on the water-water interactions than on the details of the metal-water potential function. This result is probably the cause for the similarity of the water sticking coefficient on different transition metal surfaces [1]. Although the influence of the preadsorbed molecules is not very long-ranged, the simulation results suggest that the sticking coefficient at impact energies below about 0.2 eV should be very close to unit once coverage of the surface exceeds about 0.05 to 0.1. It would be interesting to perform accurate experiments for very low coverages at hyperthermal energies to establish whether the prediction of the present work is correct.

The results show that hydrogen bonding plays indeed the important role in water adsorption that has been ascribed to it based upon the interpretation of experimental data. The existence of hydrogen bonds can be easily seen in Figure 4. It is also true, on average, that the adsorption of a molecule at low energies is coupled to a steplike decrease of the water-water interaction energy (which can be taken as a measure of the strength of hydrogen bonding). Both 2-dimensional and 3-dimensional clusters (in which molecules bind in the second layer) have been observed at slightly higher coverages (formally $\Theta = 16$) in agreement with evidence from thermal desorption spectra.

Acknowledgements

We gratefully acknowledge that this work was performed with use of grants of computer time from the University of California, Irvine on the Convex C240 and from the National Science Foundation on the CRAY YMP at the San Diego Supercomputer Center. E.S. thanks the Alexander von Humboldt Foundation for a Feodor Lynen Fellowship. P.B. thanks the Deutsche Forschungsgemeinschaft for a Heisenberg Fellowship.

[1] P. A. Thiel and Th. E. Madey, Surface Sci. Rep. **7,** 211 (1987).
[2] S. Holloway and K. H. Bennemann, Surface Sci. **101,** 327 (1980).
[3] J. E. Müller and J. Harris, Phys. Rev. Lett. **53,** 2493 (1984).
[4] M. W. Ribarsky, W. D. Luedtke, and U. Landman, Phys. Rev. B **32,** 1430 (1985).
[5] C. W. Bauschlicher, Jr., J. Chem. Phys. **83,** 3129 (1985).
[6] A. B. Anderson, Surface Sci. **105,** 159 (1981).
[7] H. Yang and J. L. Whitten, Surface Sci. **223,** 131 (1989).
[8] E. Spohr and K. Heinzinger, Ber. Bunsenges. Phys. Chem. **92,** 1358 (1988).
[9] E. Spohr, J. Phys. Chem. **93,** 6171 (1989).
[10] K. Foster, K. Raghavan, and M. Berkowitz, Chem. Phys. Lett. **162,** 32 (1989).
[11] E. Spohr, Chem. Phys. **141,** 87 (1990).
[12] P. Bopp, G. Jancsó, and K. Heinzinger, Chem. Phys. Lett. **98,** 129 (1983).
[13] J. E. Black and P. Bopp, Surface Sci. **140,** 275 (1984).
[14] H. Ibach and S. Lehwald, Surfce Sci. **91,** 187 (1980).
[15] E. Spohr, unpublished results.
[16] G. B. Fisher and J. L. Gland, Surface Sci. **94,** 446 (1980).
[17] C. W. Gear, Argonne National Laboratory Report ANL-7126, 1966. – M. P. Allen and D. J. Tildesley, Computer Simulation of Liquids, Clarendon Press, Oxford 1987.
[18] E. Spohr and M. Wolfsberg, unpublished results.
[19] J. C. Tully, J. Chem. Phys. **73,** 6333 (1980).